Development of oxide precipitates in silicon: calculation of the distribution function of the classical theory of nucleation by a nodal-points approximation

2007 J. Phys.: Condens. Matter 19 496202

(http://iopscience.iop.org/0953-8984/19/49/496202)

IOP PUBLISHING JOURNAL OF PHYSICS: CONDENSED MATTER

J. Phys.: Condens. Matter **19** (2007) 496202 (11pp) doi:10.1088/0953-8984/19/49/496202

Development of oxide precipitates in silicon: calculation of the distribution function of the classical theory of nucleation by a nodal-points approximation

J Kuběna, A Kuběna, O Caha and P Mikulík

Department of Condensed Matter Physics, Masaryk University, Kotlářská 2, CZ-61137 Brno, Czech Republic

E-mail: mikulik@physics.muni.cz

Received 14 August 2007, in final form 18 October 2007
Published 12 November 2007
Online at stacks.iop.org/JPhysCM/19/496202

Abstract

The classical theory of nucleation in solids is mathematically expressed by a system of differential equations for temporal development of cluster distribution (sizes and their concentration). Cluster sizes reach hundreds of nanometers during long annealing times, requiring us to deal with up to 10^7–10^8 differential equations. The full numerical simulation grows linearly with the number of equations, making the numerical solution extremely time-consuming. In this paper we develop a nodal-points approximation method with a logarithmic efficiency, which allows us to calculate the cluster distribution very quickly. The method is based on modified Becker–Döring equations solved precisely only within a given set of nodal points and approximated in between them. Availability of the method is shown by monitoring the kinetics of oxygen precipitation in Czochralski silicon for the case of a three-stage annealing for 8 h at 600 °C + 4 h at 800 °C + 8 h at 1000 °C, where the number of monomers in the clusters reaches more than 2×10^7. Examples are discussed, mainly about the development of a concentration gap and concentration wavelet of the cluster distribution and about interstitial oxygen concentration.

1. Introduction

Precipitation of inclusions of nanometer size is an important process, which leads to a change in the physical parameters of glasses, metals, and semiconductors. The classical theory of nucleation in liquids and glasses has been successfully developed for decades [1]. Recently it has been applied into a precipitation of oxygen in Czochralski-grown silicon monocrystals [2, 3], which has an important technological impact for microelectronics. It has been shown that the classical theory helps considerably in controlling the processes of oxygen precipitation and in gettering engineering of Si wafers. There, the basic measurable quantities

are the concentration and size of SiO_2 precipitates—clusters of oxygen monomers. Calculation of the cluster distribution as it develops in time according to a temperature treatment of the sample allows a deeper insight into the kinetics (formation and growth) of precipitates.

The classical theory is based on standard Becker–Döring (BD) equations [1] or on modified Becker–Döring equations [4]. The standard Becker–Döring nucleation equations as proposed, for example, in [1] have the property to keep the total number of clusters constant. Therefore, standard BD equations do not conserve the total number of oxygen atoms in the system, i.e. the sum of oxygen monomers in clusters and the rest of the interstitial oxygen. This drawback is withdrawn by the modified system of BD equations as in e.g. [4], which conserves the oxygen amount. This leads to a system of coupled linear differential equations for the temporal development of the cluster distribution. Depending on achievable maximal cluster size, there can be up to 10^8 equations. This enormous number of equations is the fundamental problem of the nucleation simulation. Therefore, several simplifying assumptions of nucleation kinetics have been introduced in [1, 5–7]. Another approach to solve the nucleation of huge clusters is to transform the system of ordinary differential BD equations into the partial differential Fokker–Planck equation [8]. However, the Fokker–Planck equation does not describe well the evolution of small clusters.

This paper is focused on a direct calculation of cluster size distribution from a system of modified BD nucleation equations without any other simplifying assumptions on the nucleation kinetics process. We introduce a novel approximate method which reduces the number of simultaneously solved coupled differential equations by specially selecting a limited set of cluster sizes—limited set of equations selecting a limited set of nodal points. The temporal cluster size distribution is linearized between nodal points, which leads to a considerable speed-up of the numerical simulation. The model allows for simulations of subsequent annealing processes at different temperatures. This is demonstrated by an example of a three-step annealing, similar to that of [2]: determination of oxygen precipitation in Si wafers during annealing for 8 h at 600 °C + 4 h at 800 °C + 8 h at1000 °C. The distribution function of oxygen clusters is simulated and discussed for all these stages, together with a detailed analysis of the concentration gap and concentration wavelet of the cluster distribution at the highest temperature.

2. Theory of oxygen precipitation in silicon

2.1. The classical theory of nucleation

From a thermodynamic point of view, the nucleation of oxygen precipitates starts and progresses by gathering SiO monomers into clusters of a spherical shape. The free energy W_n of a cluster with n monomers is given by [2]

$$W_n = n\Delta G' + (36\pi)^{1/3} v_1^{2/3} n^{2/3} \sigma, \tag{1}$$

where $\Delta G' = -k_B T \ln\left(c(t)/c^{eq}\right)$ is the Gibbs free energy for the volume v_1 of one monomer, n is the number of monomers in the cluster and σ is a surface energy (an effective value in the sense of equation (4.8) in [7]). The c^{eq} is interstitial oxygen concentration for a thermodynamic equilibrium at temperature T. The $c(t)$ is the concentration of interstitial oxygen at time t (it decreases from the initial value c_0 as the oxygen gets stored in the clusters).

Let us denote by $N_n(t)$ the concentration of clusters of size n (i.e. clusters of n monomers) in the sample; $N_1(t) = c(t)$. The set of time-dependent functions $\{N_n(t), n \geqslant 1\}$ describes the evolution of the complete cluster distribution from the initial state $\{N_n(0)\}$. The modified BD equations, which conserve the amount of oxygen in the sample, lead to a system of coupled

differential equations

$$\begin{aligned}
\frac{\mathrm{d}N_1}{\mathrm{d}t} &= -k_1^+ N_1 + k_2^- N_2 - \sum_{i=2}^{\nu} \left(k_i^+ - k_i^-\right) N_i \\
\frac{\mathrm{d}N_i}{\mathrm{d}t} &= k_{i-1}^+ N_{i-1} - (k_i^+ + k_i^-) N_i + k_{i+1}^- N_{i+1} \\
\frac{\mathrm{d}N_\nu}{\mathrm{d}t} &= k_{\nu-1}^+ N_{\nu-1} - (k_\nu^- + k_\nu^+) N_\nu,
\end{aligned} \tag{2}$$

where ν is the maximal size of clusters in the sample. Rates of the cluster growth k_i^+ and the cluster loss k_i^- are given by

$$\begin{aligned}
k_n^+(t) &= (4\pi)^{2/3} (3v_1 n)^{1/3}\, D\, \mathrm{e}^{-\frac{\delta W_n}{2k_\mathrm{B}T}} c(t) \\
k_{n+1}^-(t) &= (4\pi)^{2/3} (3v_1 n)^{1/3}\, D\, \mathrm{e}^{+\frac{\delta W_n}{2k_\mathrm{B}T}} c(t),
\end{aligned} \tag{3}$$

where $\delta W_n = W_{n+1} - W_n$, and D is the diffusion coefficient of the interstitial oxygen in silicon.

For theoretical consideration, a property called critical cluster size $n^*(T)$ is defined. It is given by [2]

$$n^*(T) = \frac{32\pi\sigma^3 v_1^2}{3|\Delta G'|^3} \tag{4}$$

which determines the minimal size of thermodynamically stable clusters at temperature T.

In the numerical simulation of the nucleation, the number of equations ν in the system (2) must be chosen in such a way that the largest cluster concentration and the amount of stored oxygen there is negligibly small during the whole process. This possesses the limit on the direct calculation of nucleation equations for a numerical analysis, as it is very time-consuming to solve the complete system for oxygen clusters of sizes tens to hundreds of nanometers, when ν reaches 10^7–10^8. This is the critical numerical limitation when calculation of the distribution function by classical theory is no longer efficient. Therefore, the authors of [5, 6] introduce a nucleation delay for the given temperature as an overall quantity describing a simplified nucleation process. Consequently, the growth of clusters of sizes larger than $3 \times n^*(T)$ is calculated by a simplified equation for the increase of their size (radius), see, for example, equation (8) in [2].

2.2. The nodal-points approximation of the classical theory

The system (2) represents a system of ν differential equations for time-dependent functions $N_i = N_i(t)$. Let us select a subset of equations with indices $1 = b(1) < b(2) < \cdots < b(m) = \nu$ and call $b(j)$ the nodal points. The equation for $\mathrm{d}N_{b(j)}/\mathrm{d}t$ depends on unknown $N_{b(j)\pm1}$, which we will interpolate by means of $N_{b(j\pm1)}$, see figure 1. Linear interpolation gives

$$N_i = N_{b(j)} \frac{b(j+1) - i}{b(j+1) - b(j)} + N_{b(j+1)} \frac{i - b(j)}{b(j+1) - b(j)} \tag{5}$$

for $j = 1, \ldots, m$ and $i = b(j) + 1, \ldots, b(j+1) - 1$, from where we obtain

$$N_{b(j)\pm1} = \frac{N_{b(j)}(\pm b(j \pm 1) \mp b(j) - 1) + N_{b(j\pm1)}}{\pm b(j \pm 1) \mp b(j)}. \tag{6}$$

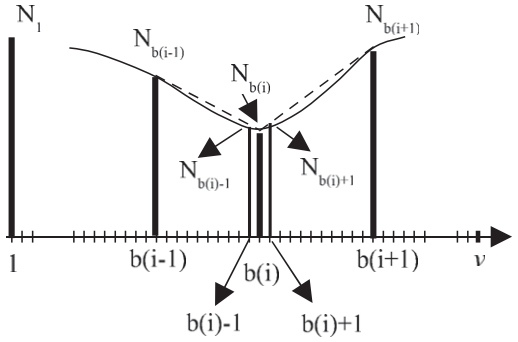

Figure 1. Scheme of the nodal-point method. The dashed lines demonstrate the linear approximation of N_j in between nodal points $b(i) < j < b(i+1)$.

This defines a reduced system of the classical theory of nucleation

$$\begin{aligned}
\frac{\mathrm{d}N_{b(1)}}{\mathrm{d}t} &= N_{b(1)}\left(-k^+_{b(1)} + k^-_{b(1)+1}\frac{b(2)-b(1)-1}{b(2)-b(1)}\right) \\
&\quad + N_{b(2)}\frac{k^-_{b(1)+1}}{b(2)-b(1)} - \sum_{j=1}^{m} N_{b(j)}\left(k^+_{b(j)} - k^-_{b(j)}\right)\frac{b(j+1)-b(j-1)}{2} \\
\frac{\mathrm{d}N_{b(j)}}{\mathrm{d}t} &= N_{b(j-1)}\frac{k^+_{b(j)-1}}{b(j)-b(j-1)} \\
&\quad + N_{b(j)}\left(k^+_{b(j)-1}\frac{b(j)-b(j-1)-1}{b(j)-b(j-1)} - k^-_{b(j)} - k^+_{b(j)}\right. \\
&\quad \left. + k^-_{b(j)+1}\frac{b(j+1)-b(j)-1}{b(j+1)-b(j)}\right) \\
&\quad + N_{b(j+1)}\frac{k^-_{b(j)+1}}{b(j+1)-b(j)} \\
\frac{\mathrm{d}N_{b(m)}}{\mathrm{d}t} &= N_{b(m-1)}\frac{-k^+_{b(m)-1}}{b(m)-b(m-1)} \\
&\quad + N_{b(m)}\left(k^+_{b(m)-1}\frac{b(m)-b(m-1)-1}{b(m)-b(m-1)} - k^-_{b(m)} - k^+_{b(m)}\right)
\end{aligned} \tag{7}$$

for $j = 2, \ldots, m-1$ and we call it the nodal-points approximation. The reduced system can be solved by standard numerical integration methods.

3. Numerical simulations of oxygen nucleation in silicon

Let us simulate a series of oxygen nucleation processes in Czochralski-grown silicon crystals. In order to facilitate mutual comparison, the material parameters utilized are the same as in [2]:

$$\begin{aligned}
&v_1 = 20.8\ \mathrm{cm}^3\ \mathrm{mol}^{-1} \\
&\sigma = 0.48\ \mathrm{J\ m}^{-2} \\
&c^{\mathrm{eq}} = 2.2\times 10^{21}\,\mathrm{e}^{-1.03\ \mathrm{eV}/k_{\mathrm{B}}T}\ \mathrm{cm}^{-3} \\
&D = \begin{cases} 2.16\times 10^{-6}\,\mathrm{e}^{-1.55\ \mathrm{eV}/k_{\mathrm{B}}T}\ \mathrm{cm}^2\ \mathrm{s}^{-1} & \text{for } T < 973\ \mathrm{K} \\ 0.13\,\mathrm{e}^{-2.53\ \mathrm{eV}/k_{\mathrm{B}}T}\ \mathrm{cm}^2\ \mathrm{s}^{-1} & \text{for } T > 973\ \mathrm{K}. \end{cases}
\end{aligned}$$

We will solve numerically the reduced system of equations (7) in nodal points which we have chosen according to this rule:

$$\begin{aligned} &b(1) = 1 \\ &b(j+1) = b(j) + \max(1, \lfloor b(j)\Delta b \rfloor) \qquad \text{for } j = 1 \ldots m-1, \end{aligned} \tag{8}$$

where Δb is a relative step between nodes. For large j the nodal points are distributed equidistantly in a logarithmic scale. We were simulating with Δb from 0.001 to 0.01.

It should be noted that the nucleation equations (7) are not strictly a system of differential equations with constant coefficients. This is because the coefficients $k^{\pm}$ depend on $c(t)$, see (3). Numerically we proved a slow time-dependence, for example, the values of $k^{\pm}$ at 1000 °C do not change significantly during 0.1 h.

Precipitate concentration $\chi(t)$ can be obtained from the cluster size distribution by

$$\chi(t) = \sum_{i=n^*}^{\nu} N_i(t) \tag{9}$$

and the concentration of the interstitial oxygen by

$$c(t) = c_0 - \Delta c(t) = c_0 - \sum_{i=2}^{\nu} \mathrm{i} N_i(t). \tag{10}$$

We will further demonstrate simulation of the distribution function $N_i(t)$ by means of the nodal-points approximation on a three-stage annealing of silicon crystals. The initial oxygen concentration is $c_0 = 8.4 \times 10^{17}$ cm^{-3} and the wafers are in an ideal initial state, when only Si–O clusters of size 1 are present. Simulation of a multi-stage annealing allows us to observe the development of the distribution function at each time during the annealing stages.

3.1. The first stage: annealing at 600 °*C*

3.1.1. Short annealing at 600 °C. The temperature of the first annealing stage has been chosen as 600 °C in order to stay in the validity of the classical nucleation theory [7]. From the simulation we can see that the distribution of cluster sizes broadens towards larger clusters during the annealing, see figure 2(a). Concentration $\chi(t)$ of clusters larger than the critical value $n^*(600\,^\circ\mathrm{C}) = 9$ increases with a stationary nucleation rate after the first 30 min. This time, called the nucleation delay, is needed to develop clusters larger than the critical size, see graph (c). On graph (b) we can see that the oxygen concentration in clusters larger than n^* is about five orders of magnitude smaller than c_0. This means that the loss of the interstitial oxygen is not measurable by a standard infrared experiment. Therefore we confirm that the coefficients $k^{\pm}$ are almost constant in time as we have stated above.

3.1.2. Long annealing at 600 °*C*. This simulation of the nucleation process at 600 °C, see figure 3, extends the annealing time of figure 2 up to 800 h. Other process properties of oxygen nucleation are clearly visible too: a slow tendency to cease the linear growth of cluster concentration, a region of saturation of the precipitate concentration (see curve on subfigure (c)), and the subsequent decrease of the interstitial oxygen concentration, which tends to the equilibrium concentration of c^{eq}.

Let us note that the annealing time of about 200 h, after which the precipitate concentration is constant, is linked to the formation of the concentration wavelet in the cluster distribution.

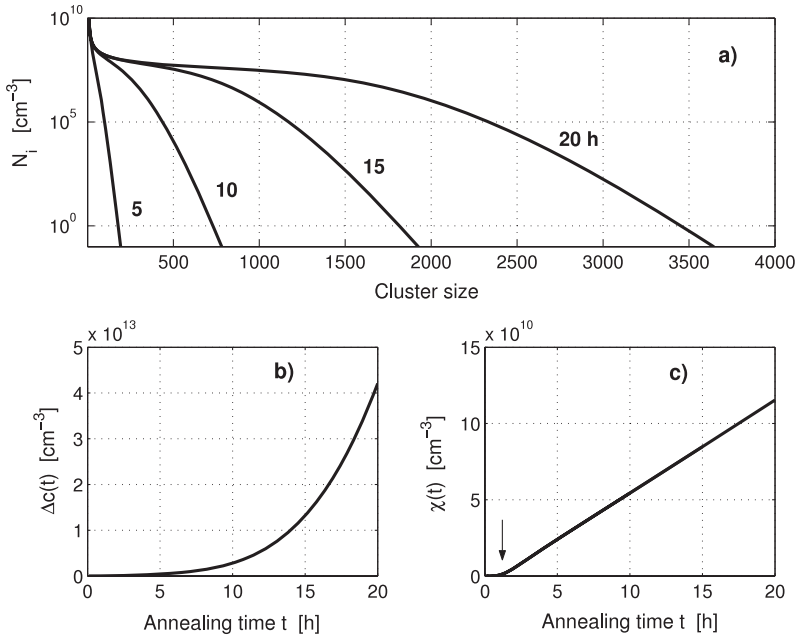

Figure 2. Simulation of annealing at 600 °C. (a) Cluster size distribution after various annealing times (in hours). (b) Oxygen concentration stored in clusters and (c) precipitate concentration. The arrow denotes the nucleation delay of 30 min.

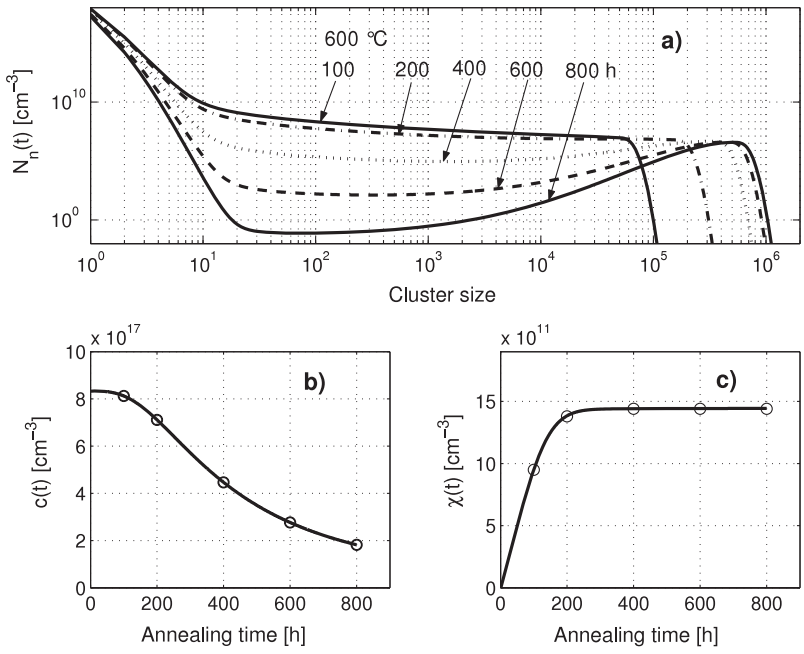

Figure 3. Simulation of long-time annealing at 600 °C, up to 800 h. (a) Cluster size distribution after various annealing times (in hours). Temporal dependence of (b) interstitial oxygen concentration and (c) cluster concentration.

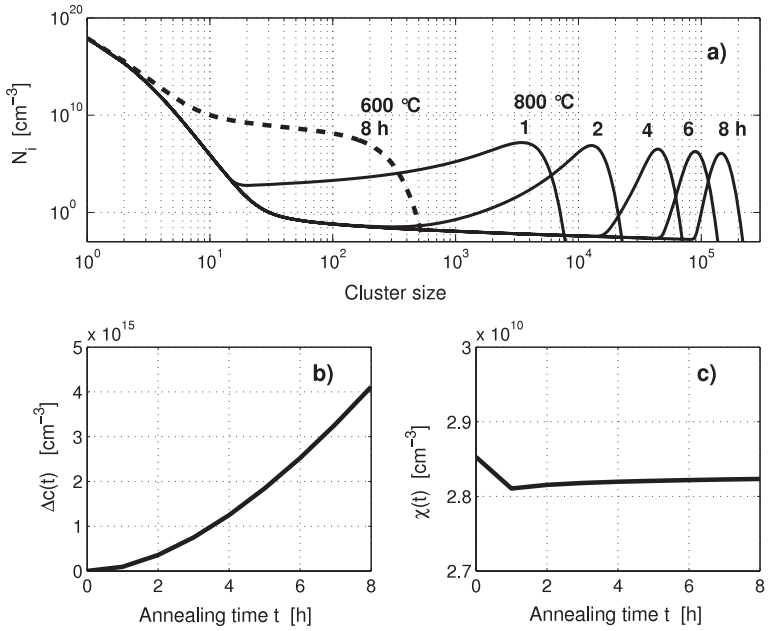

Figure 4. Simulation of an 8 h annealing at 600 °C followed by 800 °C at different durations. (a) Cluster size distribution after various annealing times (in hours). (b) Oxygen concentration stored in clusters and (c) the precipitate concentration.

3.2. The second stage: annealing at 800 °*C*

Let the second annealing stage at 800 °C follow the first annealing stage of 8 h at 600 °C. Simulation results of the time evolution are shown in figure 4. The curve labeled '8 h at 600 °C' on graph (a) is the distribution just after the first stage. This distribution enters as the initial state of the reduced system of nucleation equations (7) for temperature 800 °C.

Graph (a) shows two important features: a *concentration wavelet* develops in the cluster distribution after approximately 2 h, and a broad *concentration gap* separates small and large clusters. The wavelet shifts towards larger values, thus clusters grow and the amount of oxygen stored in them $\Delta c(t)$ increases as well. Graph (b) shows that about 0.5% of c_0 is stored in the wavelet after 8 h. On the other hand, graph (c) confirms an almost constant precipitate concentration. The value corresponds to the creation of the concentration gap (10^{-2} cm^{-2}) which separates the concentration wavelet. The gap plays an important role for a choice of temperatures for controlling the multi-stage annealing processes.

3.3. The third stage: annealing at 1000 °*C*

Let the third annealing stage at 1000 °C follow the second annealing stage of 4 h at 800 °C and the first one of 8 h at 600 °C, see figure 5. The temperature of 1000 °C is relevant in order to measure the cluster concentration $\chi(t)$ by an etching method, or to measure the interstitial oxygen loss $c(t)$ by infrared absorption.

The initial cluster distribution for annealing at 1000 °C exhibits a large concentration gap (see the dashed line in figure 5(a)). It shows that after 16 h at 1000 °C the average cluster size is 2×10^7 monomers, which corresponds to the cluster radius $r = 65$ nm.

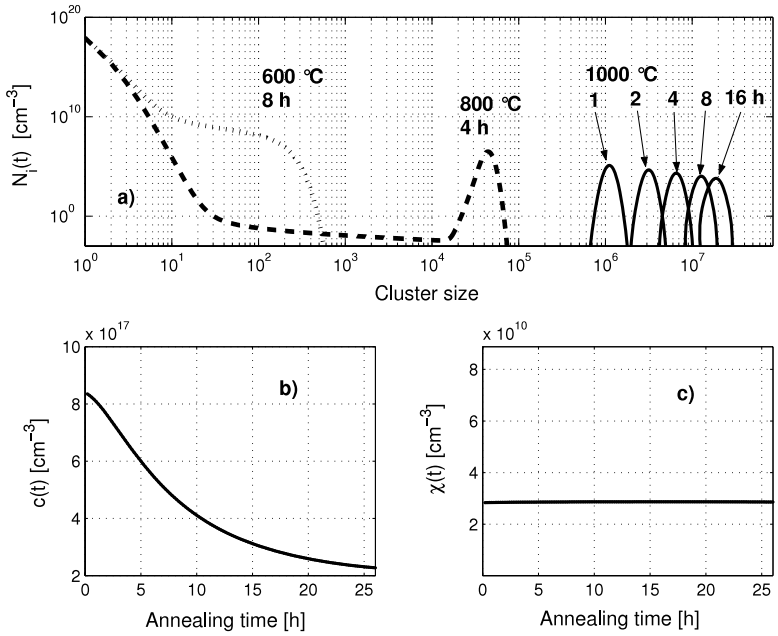

Figure 5. (a) Cluster size distribution simulation of the third annealing at 1000 °C and various durations (solid lines) after the 600 °C 8 h (dotted line) and 800 °C 4 h process (dashed line). (b) Decrease of the interstitial oxygen concentration and (c) the precipitate concentration.

Figure 6 compares two numerical simulations. Solid lines correspond to a simulation of the full BD system; the number of equations is reduced to $\nu = 5 \times 10^5$ in the wavelet region. To make the simulations faster, we did not simulate the BD equations in the region of the concentration gap, since the number of clusters in the concentration gap is negligible. However, it is necessary to respect the $k^{\pm}$ dependence on $c(t)$ exactly according to (3). Dashed lines correspond to a simulation by means of the nodal-points approximation (about 10^3 equations).

We find in figure 6(a) that the wavelet shape is different for the nodal-points approximation compared to the exact solution. However, the wavelet maximum, thus the average cluster size, does not depend on the step Δb.

We find that determination of the cluster concentration and the oxygen concentration, see figure 6(b), is more precise by the nodal-points approximation than obtained by a typical experiment. The error caused by an approximation $\Delta b = 0.001$ is smaller than 1% for the cluster concentration. Interstitial oxygen concentration $c(t)$ decreases with annealing time from 8.4×10^{17} cm^{-3} and the fully simulated and the approximated curves coincide, see graph (c).

The influence of the relative step Δb on the concentration of clusters and oxygen is presented in detail in figure 7. We find that both dependencies converge linearly towards a certain value for $\Delta b = 0$, which corresponds to the calculation according to the full system of nucleation equations (2). We have tested that the sequence of the nodal points (8) was optimal for the given simulation.

We have shown that all important quantities (mean cluster size, total cluster concentration and the interstitial oxygen concentration) are not affected by the nodal-point approximation. This result determines the practical applicability of the approximation. Its main advantage is the calculation time: simulation of the full system has taken 10 days, while the nodal-points approximation for $\Delta b = 0.001$ has taken only 1 h.

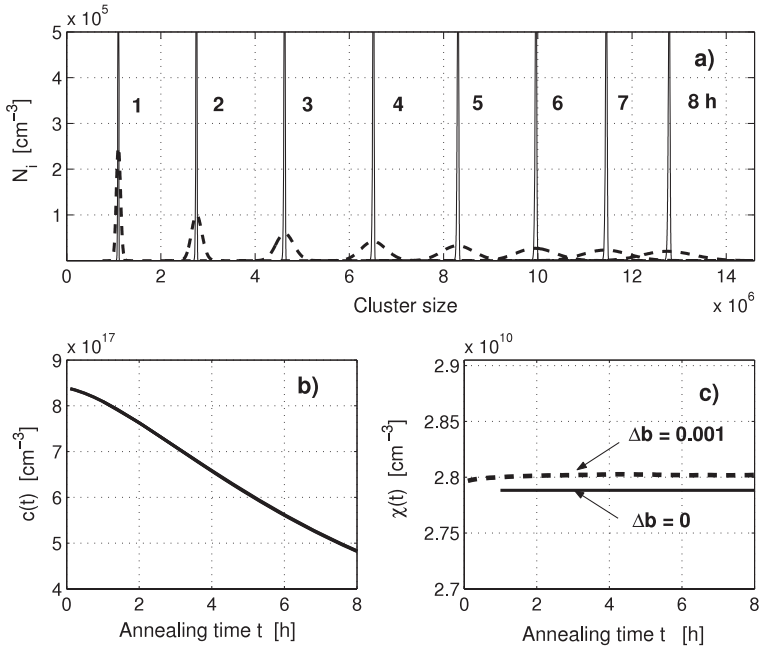

Figure 6. Simulation of the third annealing at 1000 °C for different durations. Solid lines: full system of nucleation equations (or $\Delta b = 0$), dashed lines: nodal-points approximation for $\Delta b = 0.001$.

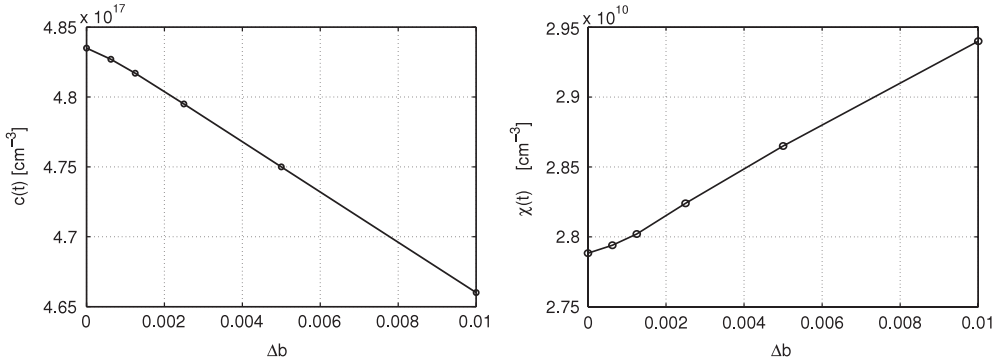

Figure 7. Dependence of the oxygen concentration $c(t = 8\text{ h})$ (left) and the cluster concentration $\chi(t = 8\text{ h})$ (right) in the concentration wavelet on relative distance Δb of the nodes. The simulation corresponds to the third annealing stage of 8 h at 1000 °C.

4. Discussion

In this paper, we have demonstrated that the nodal-points approximation is fully functional for the modified system of BD equations. Then, it is possible to simulate a single precipitation process for an arbitrarily long processing time, as it completely describes all three parts of the nucleation process: nucleation delay, stationary growth of clusters, and the saturation of cluster concentration, see figures 2 and 3. Let us note that Ham's theory of precipitation [9] can only be applied for the annealing time in the region of saturation, figure 3.

The modified system of BD equations and their solution via the nodal-points method can be used to study nucleation during multi-stage processes involving both heating and cooling, as well as kinetics of annealing processes with changing temperature. This topic will be the subject of our next study.

From figure 4 it follows that the distribution function for cluster sizes 1 to approximately 100 monomers no longer changes after a certain time and similarly for the concentration gap separating the concentration wavelet. Therefore the number of clusters in the wavelet is conserved during the subsequent annealing. Such a mechanism of a three-stage annealing is qualitatively described in [10]. By a detailed study of the development of the distribution function at different temperatures we can find simple relationships, e.g. between the stationary growth rate and the displacement rate of the concentration wavelet.

From the point of view of the classical theory of nucleation, there is a permanent process of growth and dissolution of clusters, regardless of their size, even for clusters much larger than their critical size. The growth of precipitates can be considered as a continuation of nucleation, when the dissolution rate is small. The system of nucleation equations can therefore be used to study precipitation processes, which are often studied individually, only as a diffusion-driven precipitation based on the Ham theory [9].

Considering the oxygen precipitation process there are still open questions about transformation of clusters of oxygen monomers into clusters of SiO_2 molecules. It was discussed in [3, 10, 11], mainly in conjunction with the discontinuity of the diffusion coefficient of oxygen with temperature. These open problems of the precipitation of oxygen in silicon can only be solved in interpretation with reproducible experimental data for $c(T, t)$ and $\chi(T, t)$ by the classical nucleation theory. This can be a way of determining more exactly the surface energy $\sigma(T)$ and clarifying the discontinuity in the oxygen diffusion constant $D(T)$.

5. Conclusion

In this paper, we have theoretically studied and simulated cluster distribution, based on the classical theory of nucleation, expressed by modified Becker–Döring equations. For their solution we succeeded in formulating a nodal-points approximation, which considerably reduced the number of differential equations solved simultaneously. Our approach substantially reduces the computing time needed to simulate the distribution functions compared to the complete solution.

We have demonstrated the method of simulating nucleation and precipitation of oxygen during a three-stage annealing in Czochralski-grown silicon. We have shown that it is possible to obtain values with a sufficient precision (1–3% according to the value of Δb) for the precipitate concentration and the time-dependence of the concentration of the remnant interstitial oxygen, which are the two experimentally observable quantities.

Acknowledgments

The authors acknowledge support by the Ministry of Education of the Czech Republic (grant MSM 0021622410). One of us (OC) was also supported by the Grant Agency of the Academy of Sciences of the Czech Republic (GAAV) grant B101630601.

References

[1] Kelton K F 1991 Crystal nucleation in liquids and glasses *Solid State Phys.* **45** 75–177
[2] Kelton K F 1999 Oxygen precipitation in silicon: experimental studies and theoretical investigations within classical theory of nucleation *J. Appl. Phys.* **85** 8097–111

[3] Wei P F, Kelton K F and Falster R 2000 Coupled-flux nucleation modeling of precipitation in silicon *J. Appl. Phys.* **88** 5062–70
[4] Niethammer B 2003 On the evolution of large clusters in the Becker–Döring model *J. Nonlinear Sci.* **13** 115–55
[5] Kelton K F, Greer A L and Thompson C V 1983 Transient nucleation in condensed system *J. Chem. Phys.* **79** 6261–76
[6] Ranasinghe K S, Wei P F, Kelton K F, Ray C S and Day D E 2004 Verification of analytical method for measuring crystal nucleation rates of glasses from DTA data *J. Non-Cryst. Solids* **337** 261–7
[7] Kelton K F 2003 Diffusion-influenced nucleation: a case study of oxygen precipitation in silicon *Phil. Trans. R. Soc.* A **361** 429–46
[8] Ko B G and Kwack K D 1999 Growth/dissolution model for oxygen precipitation based on the kinetics of phase trasformations *J. Appl. Phys.* **85** 2100–7
[9] Ham F S 1958 Theory of diffused-limited precipitation *J. Phys. Chem. Solids* **6** 335–51
[10] Falster R, Cornara M, Gambaro D, Olmo M and Pagani M 1997 Effect of high temperature pre-anneal on oxygen precipitates nucleation kinetics in Si *Solid State Phenom.* **57/58** 123–8
[11] Newman R C 2000 Oxygen diffuson and precipitation in Czochralski silicon *J. Phys.: Condens. Matter* **12** 335–65